

# Adaptive Pairwise Encodings for Link Prediction

Harry Shomer  
shomerha@msu.edu  
Michigan State University  
East Lansing, USA

Juanhui Li  
lijuanh1@msu.edu  
Michigan State University  
East Lansing, USA

Yao Ma  
may13@rpi.edu  
Rensselaer Polytechnic Institute  
Troy, USA

Bo Wu  
bwu@mines.edu  
Colorado School of Mines  
Golden, USA

Haitao Ma  
haitaoma@msu.edu  
Michigan State University  
East Lansing, USA

Jiliang Tang  
tangjili@msu.edu  
Michigan State University  
East Lansing, USA

## ABSTRACT

Link prediction is a common task on graph-structured data that has seen applications in a variety of domains. Classically, hand-crafted heuristics were used for this task. Heuristic measures are chosen such that they correlate well with the underlying factors related to link formation. In recent years, a new class of methods has emerged that combines the advantages of message-passing neural networks (MPNN) and heuristics methods. These methods perform predictions by using the output of an MPNN in conjunction with a “pairwise encoding” that captures the relationship between nodes in the candidate link. They have been shown to achieve strong performance on numerous datasets. However, current pairwise encodings often contain a strong inductive bias, using the same underlying factors to classify all links. This limits the ability of existing methods to learn how to properly classify a variety of different links that may form from different factors. To address this limitation, we propose a new method, **LPFormer**, which attempts to adaptively learn the pairwise encodings for each link. LPFormer models the link factors via an attention module that learns the pairwise encoding that exists between nodes by modeling multiple factors integral to link prediction. Extensive experiments demonstrate that LPFormer can achieve SOTA performance on numerous datasets while maintaining efficiency.

## CCS CONCEPTS

• **Computing methodologies** → **Machine learning**.

## KEYWORDS

link prediction, graph transformer

## ACM Reference Format:

Harry Shomer, Yao Ma, Haitao Ma, Juanhui Li, Bo Wu, and Jiliang Tang. 2018. Adaptive Pairwise Encodings for Link Prediction. In *Woodstock '18: ACM Symposium on Neural Gaze Detection, June 03–05, 2018, Woodstock, NY*. ACM, New York, NY, USA, 14 pages. <https://doi.org/XXXXXXXX.XXXXXXX>

Permission to make digital or hard copies of all or part of this work for personal or classroom use is granted without fee provided that copies are not made or distributed for profit or commercial advantage and that copies bear this notice and the full citation on the first page. Copyrights for components of this work owned by others than ACM must be honored. Abstracting with credit is permitted. To copy otherwise, or republish, to post on servers or to redistribute to lists, requires prior specific permission and/or a fee. Request permissions from [permissions@acm.org](mailto:permissions@acm.org).  
*Conference'17, July 2017, Washington, DC, USA*

© 2018 Association for Computing Machinery.  
ACM ISBN 978-1-4503-XXXX-X/18/06...\$15.00  
<https://doi.org/XXXXXXXX.XXXXXXX>

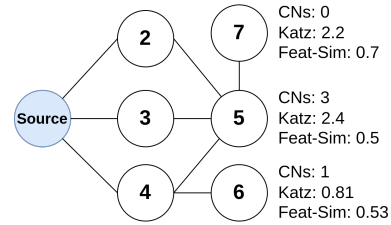


**Figure 1: Example of multiple heuristic scores for the candidate links (source, 5), (source, 6), and (source, 7). Each heuristic corresponds to a different LP factor – local (CNs), global (Katz), and feature proximity (Feat-Sim).**

## 1 INTRODUCTION

Link prediction (LP) attempts to predict unseen edges in a graph. It has been adopted in many applications including recommender systems [20], social networks [13], and drug discovery [1]. Traditionally, hand-crafted heuristics were used to identify new links in the graph [2, 33, 49]. Heuristics are often chosen based on factors that typically correlate well with the formation of new links. For example, a popular heuristic is common neighbors (CNs), which assume that the links are more likely to exist between node pairs with more shared neighbors. It’s been found that these factors, which we refer to as “LP Factors”, often stem from the local and global structural information and feature proximity [29]. We give an example in Figure 1 that shows different heuristic scores for multiple candidate links. Each heuristic score corresponds to one of the LP factors: CNs for local information, Katz for global, and Feat-Sim for feature proximity. We can observe that the pair (source, 5) has the highest CN and Katz score of the candidate links, indicating an abundance of local and global structural information between the pair. On the other hand, the feature similarity for (source, 5) is the lowest among the candidate links. This indicates that different LP factors and heuristics have differing assumptions about why links are formed.

More recently, message passing neural networks [16] (MPNNs), which are able to learn effective node representations with message-passing mechanisms, have been widely adopted for LP tasks. They predict the existence of a link by combining the node representations of both nodes in the link. However, such a node-centric view is unable to incorporate the pairwise information between the nodes in the link. Because of this, conventional MPNNs have been

demonstrated to be poor link predictors due to their limited capability to learn effective and expressive link representations [37, 46]. To address this issue, recent efforts [45, 50] have attempted to move beyond the node-centric view of traditional MPNNs by equipping them with pairwise information specific to the link being predicted (i.e. the “target link”). This is done by customizing the message passing process to each target link. For example, SEAL [45] first extracts the  $k$ -hop subgraph around each target link and then initializes the nodes with features that describe their relationship with the target link. Message passing is correspondingly run on this subgraph, with the pooled node representations being used for prediction. It has been shown that SEAL, along with a related method NBFNet [50], can learn many LP heuristics such as common neighbors [33] and Katz [21]. However, a concern with this approach is that it can be prohibitively expensive [9], as message passing needs to be run for each individual target link. This is as opposed to traditional MPNNs which only run message passing once for all target links.

To overcome these inefficiencies, recent methods [9, 40, 44] have instead explored ways to inject pairwise information into the model, without individualizing the message passing to each target link. This is done by decoupling the message passing and link-specific pairwise information. By doing so, the message passing only needs to be done once for all target links. To include pairwise information, these methods, which we refer to as “Decoupled Pairwise MPNNs” (DP-MPNNs), instead learn a “pairwise encoding” to encode the pairwise relationship of the target link. The choice of pairwise encoding is often based on heuristics that correspond to common LP factors (e.g., common neighbors). DP-MPNNs have gained attention as they can achieve promising performance while being much more efficient than methods that customize the message passing mechanism.

However, DP-MPNNs are often limited in the choice of pairwise encoding, using a one-size-fits-all solution for all target links. This has two important limitations. (1) The pairwise encoding may fail to consider some integral LP factors. For example, NCNC [40] only considers the 1-hop neighborhood when computing the pairwise encoding, thereby ignoring the global structural information. *This suggests the need for a pairwise encoding that considers multiple types of LP factors.* (2) The pairwise encoding uses the same LP factors for all target links. This assumes that all target links need the same factors. However, this may not necessarily be true. Recently, Mao et al. [29] have shown that different LP factors are necessary to classify different target links. This tells us that even for the same dataset, multiple LP factors are needed to properly predict all target links. This further applies to different datasets, where certain factors are more prominent than others. As such, it is vital to be careful when considering multiple types of LP factors. While one factor may effectively model some target links, it will fail for other target links where those patterns aren’t present. *It is therefore desired to consider different LP factor(s) for different target links.*

These observations motivate us to ask – *can we design an efficient method that can adaptively determine which LP factors to incorporate for each individual target link?* This requires a pairwise encoding that (a) models multiple LP factors, (b) can be tailored to fit each individual target link, and (c) is efficient to calculate. By doing so, we can flexibly adapt the pairwise information based on the existing needs of each target link. To achieve this, we propose

**LPFormer – Link Prediction TransFormer.** LPFormer is a type of graph Transformer [31] designed specifically for link prediction. Given a target link  $(a, b)$ , LPFormer models the pairwise encoding via an attention module that learns how  $a$  and  $b$  relate in the context of various LP factors. This allows for a more customizable set of pairwise encodings that are specific to each target link. Extensive experiments validate that LPFormer can achieve SOTA on a variety of benchmark datasets. We further demonstrate that LPFormer is better at modeling several types of LP factors, highlighting its adaptability, while also maintaining efficiency on denser graphs.

## 2 BACKGROUND

### 2.1 Related Work

Link prediction (LP) aims to model how links are formed in a graph. The process by which links are formed, i.e., link formation, is often governed by a set of underlying factors [5, 28]. We refer to these as “LP factors”. Two categories of methods are used for modeling these factors – heuristics and MPNNs. We describe each class of methods. We further include a discussion on existing graph transformers.

**Heuristics for Link Prediction.** Heuristics methods [33, 49] attempt to explicitly model the LP factors via hand-crafted measures. Recently, Mao et al. [29] have shown that there are three main factors that correlate with the existence of a link: (1) local structural information, (2) global structural information, and (3) feature proximity. **Local structural information** only considers the immediate neighborhood of the target link. Representative methods include Common Neighbors (CN) [33], Adamic Adar (AA) [2], and Resource Allocation (RA) [49]. They are predicated on the assumption that nodes that share a greater number neighbors exhibit a higher probability of forming connections. **Global structural information** further considers the global structure of the graph. Such methods include Katz [21] and Personalized PageRank (PPR) [6]. These methods posit that nodes interconnected by a higher number of paths are deemed to have larger similarity and, therefore, are more likely to form connections. Lastly, **feature proximity** assumes nodes with more similar features connect [32]. Previous work [34, 48] have shown that leveraging the node features are helpful in predicting links. Lastly, we note that Mao et al. [29] has recently shown that *to properly predict a wide variety of links, it’s integral to incorporate all three of these factors.*

**MPNNs for Link Prediction.** Message Passing Neural Networks (MPNNs) [16] aim to learn node representations via the message passing mechanism. Traditional MPNNs have been used for LP including GCN [23], SAGE [17], and GAE [24]. However, they have been shown to be suboptimal for LP as they aren’t expressive enough to capture important pairwise patterns [37, 47]. SEAL [45] and NBFNet [50] try to address this by customizing the message passing process to each target link. This allows for the message passing to learn pairwise information specific to the target link. However, these methods have been shown to be unduly expensive as they require a separate round of message passing for each target link. As such, recent methods have been proposed to instead decouple the message passing and pairwise information [9, 40, 44], reducing the time needed to do message passing. Such methods

include NCN/NCNC [40] which exploit the common neighbor information and BUDDY [9] and Neo-GNN [44] which consider the global structural information.

**Graph Transformers.** Recent work has attempted to extend the original Transformer [38] architecture to graph-structured data. Graphormer [43] learns node representations by attending all nodes to each other. To properly model the structural information, they propose to use multiple types of structural encodings (i.e., structural, centrality, and edge). SAN [26] further considers the use of the Laplacian positional encodings (LPEs) to enhance the learnt structural information. Alternatively, TokenGT [22] considers all nodes and edges as tokens in the sequence when performing attention. Due to the large complexity of these models, they are unable to scale to larger graphs. To address this, several graph transformers [10, 41] have been proposed for node classification that attempt to efficiently attend to the graph. However, to our knowledge, there are no graph transformers designed specifically for LP.

## 2.2 Preliminaries

We denote a graph as  $\mathcal{G} = \{\mathcal{V}, \mathcal{E}\}$ , where  $\mathcal{V}$  and  $\mathcal{E}$  are the sets of nodes and edges in  $\mathcal{G}$ , respectively. The adjacency matrix is represented as  $A \in \mathbb{R}^{|\mathcal{V}| \times |\mathcal{V}|}$ . The  $d$ -dimensional node features are represented by the matrix  $X \in \mathbb{R}^{|\mathcal{V}| \times d}$ . The set of neighbors for a node  $v$  is given by  $\mathcal{N}(v)$ . The set of overlapping neighbors between two nodes  $a$  and  $b$ , i.e., the common neighbors (CNs), is expressed by  $\mathcal{N}_{(a,b)}^{\text{CN}}$ . We further denote the set of nodes that are 1-hop neighbors of only one of  $a$  or  $b$  as  $\mathcal{N}_{(a,b)}^1$  and the nodes that are  $>1$ -hop from both nodes as  $\mathcal{N}_{(a,b)}^{>1}$ . Lastly, the personalized pagerank (PPR) score for a root node  $v$  and an arbitrary node  $u$  is given by  $\text{ppr}(v, u)$ .

## 3 THE PROPOSED FRAMEWORK

In Section 1, we highlighted the importance of adaptively modeling multiple types of LP factors. However, current methods that use pairwise encodings, i.e., DP-MPNNs, struggle to appropriately achieve this goal. This is due to two issues: **(1)** They only attempt to model a subset of the potential LP factors (e.g., only local structural information), limiting their ability to model multiple factors. **(2)** They use a one-size-fits-all approach in regard to pairwise encoding, using the same combination of LP factors for each target link. These issues strongly limit the potential of such methods to properly model a variety of different target links. To overcome these problems, we propose **LPFormer**, a new transformer-based method that can adaptively customize the pairwise information for each target link by considering variety of different LP factors in an efficient manner.

### 3.1 A General View of Pairwise Encodings

Recent MPNNs for LP use a decoupled strategy to include the pairwise information [9, 40, 44]. These methods, DP-MPNNs, predict the existence of a link  $(a, b)$  via both the node representations and a pairwise encoding  $s(a, b)$ . They follow the formulation below:

$$H = \text{MPNN}(A, X),$$

$$p(a, b) = \sigma \left( \text{MLP} \left( \mathbf{h}_a \odot \mathbf{h}_b \parallel s(a, b) \right) \right), \quad (1)$$

where  $h_i$  is the representation of node  $i$  encoded by the MPNN. Various DP-MPNNs adopt different ways to model the pairwise encoding. For example, NCN [40] models the pairwise encoding  $s(a, b)$  as the summation of the node representations of the CNs. The definitions of  $s(a, b)$  for other prominent DP-MPNNs can be found in Appendix A. The pairwise encodings in these existing methods are typically manually selected or extracted from the graph, which limits the LP factors they can cover. For example,  $s(a, b)$  in NCN and NCNC only capture the local structural information. BUDDY [9] ignores the node features when computing the pairwise encoding. To flexibly model multiple types of LP factors, we propose a general formulation for pairwise encodings as follows,

$$s(a, b) = \sum_{u \in \mathcal{V}} w(a, b, u) \odot h(a, b, u), \quad (2)$$

where  $w(a, b, u)$  measures the importance of node  $u$  to  $(a, b)$ , and  $h(a, b, u)$  is the encoding of node  $u$  relative to  $(a, b)$ . By considering *which* nodes should be considered for  $(a, b)$  and *how* they are related to the node pair, Eq. (2) can model different LP factors by manually defining  $w(a, b, u)$  and  $h(a, b, u)$ . In particular, we demonstrate how the heuristic methods corresponding to different LP factors can fit into this framework.

**Common Neighbors (CNs)** [33]: CNs considers the local structural information and is defined for a pair of nodes  $(a, b)$  as  $\mathcal{N}_{(a,b)}^{\text{CN}} = \mathcal{N}(a) \cap \mathcal{N}(b)$ . Eq. (2) is equal to the CNs when  $h(a, b, u) = 1$  and:

$$w(a, b, u) = \begin{cases} 1, & \text{when } u \in \mathcal{N}(a) \cap \mathcal{N}(b) \\ 0, & \text{else} \end{cases}. \quad (3)$$

**Katz Index** [21]: The Katz index models the global structural information. It is defined as weighted summation of the number of paths of different lengths connecting  $a$  and  $b$  and a decay weight  $\beta \in [0, 1]$ ,

$$\text{Katz}(a, b) = \sum_{l=1}^{\infty} \beta^l A_{a,b}^l.$$

This is equivalent to Eq. (2) where  $w(a, b, u) = \sum_{l=1}^{\infty} \beta^l e_a^T A^l$  and

$$h(a, b, u) = \begin{cases} e_b^T, & \text{when } u = b \\ 0, & \text{else} \end{cases},$$

where  $e_i \in \mathbb{B}^{|\mathcal{V}|}$  is a one-hot vector for a node  $i$ .

**Feature Similarity:** The feature similarity of the pair of nodes  $(a, b)$  is expressed by  $\text{dis}(\mathbf{x}_a, \mathbf{x}_b)$  where  $\mathbf{x}_a$  are the node features of node  $a$  and  $\text{dis}(\cdot)$  is a distance function (e.g., euclidean distance). This can be rewritten as Eq. (2) by substituting  $w(a, b, u) = \text{dis}(\mathbf{x}_a, \mathbf{x}_u)$  and  $h(a, b, u) = e_b^T$ .

These examples demonstrate that the general formulation can indeed model many different LP factors including local and global structural information and feature proximity. We further show in Appendix B that Eq. (2) can model a variety of additional LP factors including RA [49], the pairwise encodings used in NCN/NCNC [40] and Neo-GNN [44]. However, fitting these methods into the formulation in Eq. 2 requires manually defining both  $w(a, b, u)$  and  $h(a, b, u)$ . The constrains the information represented by  $s(a, b)$  based on the choice of design. Motivated by this, in the next section we introduce our method that does not rely on a handcrafting both  $w(a, b, u)$  and  $h(a, b, u)$ .

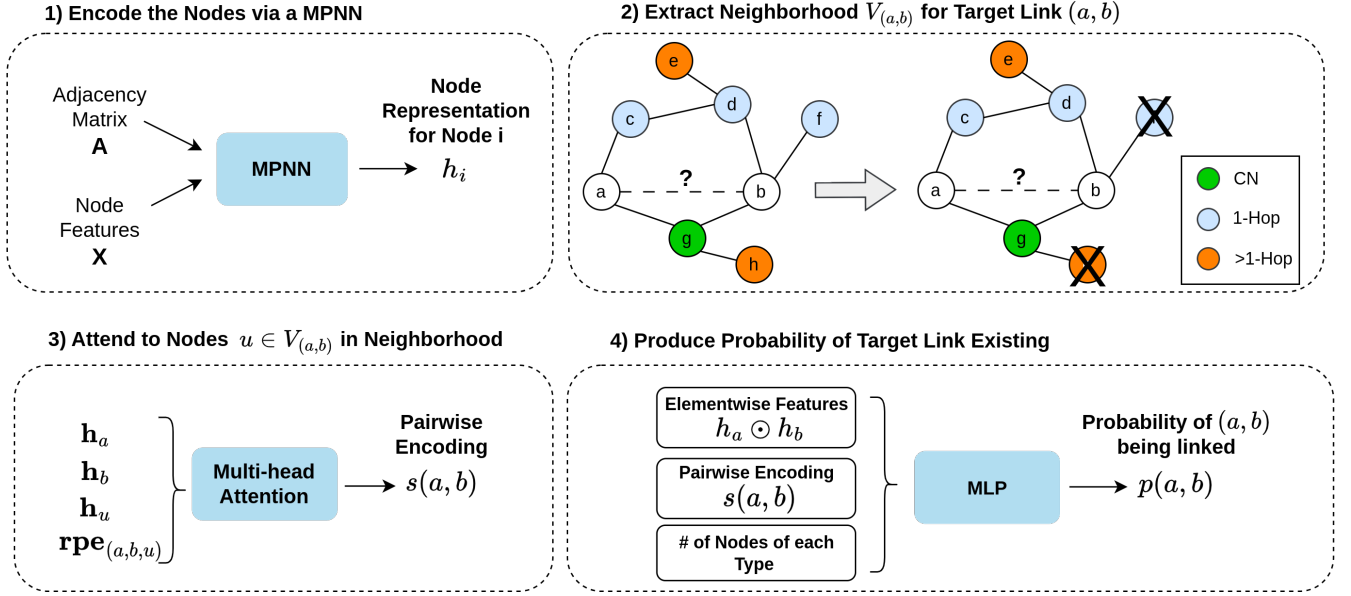


**Figure 2: An overview of LPFormer.** 1) Encode the nodes via a MPNN. 2) For a given target link, we determine which nodes to attend to ( $V_{(a,b)}$ ) via the PPR-based thresholding technique in Eq. (9). 3) The pairwise encoding is computed by attending to each node,  $u \in V_{(a,b)}$  using the feature and relative positional encoding  $\mathbf{rpe}_{(a,b,u)}$ . 4) The pairwise encoding, node representations, and counts of different node types are concatenated and used to compute the final probability of the target link existing.

### 3.2 Modeling Pairwise Encodings via Attention

In Section 3.1, we introduced a general formulation for pairwise encodings in Eq. (2), which is able to capture a variety of different LP factors. In this subsection, we further aim to move beyond a one-size-fits-all pairwise encoding, and enable the model to produce customized pairwise encoding for each target link. This allows the model to handle more realistic graphs that often contain multiple prominent LP factors as shown in [29].

In particular, we consider the following question: *How can we model Eq (2) such that it can customize the used LP factors to each target link?* We consider parameterizing both  $w(a, b, u)$  and  $h(a, b, u)$ . This allows us to learn how to personalize them to each target link. To achieve this, we leverage softmax attention [4]. This is due to its ability to dynamically learn the relevance of different nodes to the target link. As such, for multiple target links, it can emphasize the contributions of different nodes, thereby flexibly modeling different LP factors. We note that since the attention is between different sequences (i.e., a target link and nodes), it can be considered a form of cross attention [38].

To enhance the adaptability of pairwise encoding for various links, it is essential to incorporate various types of information. This allows the attention mechanism to discern and prioritize relevant information for each target link, facilitating the effective modeling of diverse LP factors. In particular, we consider two types of information. The first is the **feature information**. This includes the feature representation of both nodes in the target link and the node being attended to. The node features are included due to their role in link formation and relationship to structural information [32]. Second, we consider the **relative positional information**. The

relative positional information reflects the relative position in the graph of a node  $u$  to the target link  $(a, b)$  in the local and global structural context. Due to the importance of local and global structural information [14, 19], it is vital to properly encode both. By including both the structural and feature information, we are able to cover the space of potential LP factors (see Section 2.1).

We denote the feature representation of a node  $u$  as  $\mathbf{h}_u$  and the relative positional encoding (RPE) as  $\mathbf{rpe}_{(a,b,u)}$ . The node importance  $w(a, b, u)$  is modeled via attention as follows:

$$\begin{aligned} \tilde{w}(a, b, u) &= \phi(\mathbf{h}_a, \mathbf{h}_b, \mathbf{h}_u, \mathbf{rpe}_{(a,b,u)}), \\ w(a, b, u) &= \frac{\exp(\tilde{w}(a, b, u))}{\sum_{v \in \mathcal{V}(a,b)} \exp(\tilde{w}(a, b, v))}, \end{aligned} \quad (4)$$

where  $\mathcal{V}(a, b) = \mathcal{V} \setminus \{a, b\}$ . The attention weight  $w(a, b, u)$  can be considered as the impact of a node  $u$  on  $(a, b)$  relative to all nodes in  $\mathcal{G}$ . This allows the model to emphasize different LP factors for each target link. The node encoding  $h(a, b, u)$  includes the features of node  $u$  in conjunction with the RPE and is defined as:

$$h(a, b, u) = \mathbf{W} \left[ \mathbf{h}_u \parallel \mathbf{rpe}_{(a,b,u)} \right]. \quad (5)$$

By substituting Eq. (4) and Eq. (5) into Eq. (2) we can compute the pairwise information  $s(a, b)$ . We further define  $\phi(\cdot)$  in Eq. (4) as the GATv2 [8] attention mechanism. The feature representations  $\mathbf{h}_i$  are computed via a MPNN. We use GCN [25] in this work. However, it is unclear how to properly encode the RPE of a node  $u$  relative to  $(a, b)$ ,  $\mathbf{rpe}_{(a,b,u)}$ . We aim to design the RPE to capture both the local and global structural relationship between the node and target link while also being efficient to calculate. In the next section, we discuss our solution for modeling  $\mathbf{rpe}_{(a,b,u)}$ .

### 3.3 PPR-Based Relative Positional Encodings

In this section, we introduce our strategy for computing the RPE of a node  $u$  relative to a target link  $(a, b)$ . Intuitively, we want the RPE to reflect the positional relationship between  $u$  and  $(a, b)$  such that different types of information (i.e., local vs. global) are encoded differently. Using Figure 1 as an example, since node 3 is a CN of (source, 5) we expect it to have a much different relationship to the target link than node 6, which is a 2-hop neighbor of both nodes. An enticing option is to use the double radius node labeling (DRNL) trick introduced by Zhang and Chen [45]. However, Chamberlain et al. [9] have shown it to be prohibitively expensive to calculate for larger graphs. Furthermore, existing RPEs are typically infeasible to calculate on larger graphs as they often rely on pairwise distances or the eigenvectors of the Laplacian [36].

As such, we seek an RPE that can both distinguish the relationship of different nodes to the target link while also being efficient to calculate. To motivate our RPE design, we draw inspiration from the following Proposition.

**Proposition 1.** *Consider a target link  $(a, b)$  and a node  $u \in \mathcal{V} \setminus \{a, b\}$ . The PPR [6] score of a root node  $i$  and target node  $j$  with teleportation probability  $\alpha$  is denoted by  $\text{ppr}(i, j)$ . Let  $r_a^k(u)$  be the number of walks of length  $k$  that begin at node  $a$  and terminate at  $u$ . We define  $r_{a,b}^k(u) := r_a^k(u) + r_b^k(u)$ . We also define a weight  $\gamma^k := \alpha(1 - \alpha)^k$  for all walks of length  $k$ . The PPR scores,  $\text{ppr}(a, u)$  and  $\text{ppr}(b, u)$ , along with the aggregate number of walks of disparate lengths, are interconnected through the following relationship.*

$$\Gamma(a, b, u) = \text{ppr}(a, u) + \text{ppr}(b, u) = \sum_{k=0}^{\infty} \alpha(1 - \alpha)^k r_{a,b}^k(u). \quad (6)$$

The detailed proof is given in Appendix C. From Proposition 1, we can make the following observations: (1) The PPR scores encode the weighted sum of the number of walks between two nodes. (2) Walks of shorter length are given higher importance, as evidenced by the dampening factor  $\gamma^k = \alpha(1 - \alpha)^k$  which decays with the increase in  $k$ . These observations imply that – **a larger value of  $\Gamma(a, b, u)$  correlates with the existence of many shorter walks connecting node  $u$  to the both nodes in the target link  $(a, b)$ .**

These observations suggest that the PPR score can be used as an intuitive and useful method to understand the structural relationship between node  $u$  and both nodes in the target link  $(a, b)$ . If both scores,  $\text{ppr}(a, u)$  and  $\text{ppr}(b, u)$ , are high, there exist many shorter walks connecting  $u$  to both nodes in the target link. This implies that node  $u$  has a stronger impact on the nodes in the target link. On the other hand, if both PPR scores are low, there is likely very little relationship between  $u$  and the target link. This allows for a convenient way of differentiating how a node structurally relates to the target link. Furthermore, we note that the PPR matrix can be efficiently pre-computed using the algorithm introduced by Andersen et al. [3], allowing for easy computation and use.

Following this idea, to calculate the RPE of a node  $u$ , we use the PPR scores of a node  $u$  relative to both nodes in the target link  $(a, b)$ . Instead of considering the sum of PPR scores as in Proposition 1, we further parameterize  $\Gamma(\cdot)$  via an MLP,

$$\text{rpe}_{(a,b,u)} = \text{MLP}(\text{ppr}(a, u), \text{ppr}(b, u)). \quad (7)$$

By introducing learnable parameters to  $\Gamma(\cdot)$ , it allows for the model learn the importance of individual PPR scores and how they interact with each other. To ensure that Eq. (7) is invariant to the order of the nodes in the target link, i.e.,  $(a, b)$  and  $(b, a)$ , we further set the RPE to be equal to the summation of the representations given by both  $(a, b)$  and  $(b, a)$ :

$$\text{rpe}_{(a,b,u)} = \text{rpe}_{(a,b,u)} + \text{rpe}_{(b,a,u)}. \quad (8)$$

However, a concern with Eq. (8) is that it is not guaranteed to be able to distinguish certain types of nodes from each other. For example, it is necessary to clearly distinguish CNs from other nodes due to their important role in link formation [33]. To overcome this issue, we fit three separate MLPs for when  $u$  is a: CN of  $(a, b)$ , a 1-hop neighbor of either  $a$  and  $b$ , and a  $>1$ -hop neighbor of both  $a$  and  $b$ . This ensures that we can properly distinguish between these three types of nodes. We verify the effectiveness of this design in Section 4.4.

### 3.4 Efficiently Attending to the Graph Context

The proposed attention mechanism in Section 3.2 attends to all nodes in the graph, sans those in the link itself. This makes it difficult to scale to large graphs. Motivated by selective [30] and sparse [12] attention, we opt to attend to only a small portion of the nodes.

*How do we determine which nodes to attend to?* Existing methods like NCNC only attend to the enclosed 1-hop neighborhood of the target link. However, this has the potential to ignore vital information to the link. Depending on the type of graph and link, nodes outside the 1-hop radius of the target link may be crucial. On the other hand, SEAL uses the enclosed  $k$ -hop neighborhood. Due to the exponential increase in nodes as  $k$  increases, using  $k > 1$  on larger graphs is infeasible. We therefore desire the flexibility of being able to attend to important non-local nodes while avoiding the inclusion of too many nodes.

In Proposition 1, we demonstrate that the PPR score between the node pair  $(a, u)$  can be interpreted as the weighted number of walks from  $a$  to  $u$ . As such, a higher PPR score indicates that more walks of shorter length tend to connect the pair of nodes, indicating a stronger structural relationship. This concept is used to formulate the RPE in Section 3.3. However, *what if the PPR score of node  $u$  is low compared to both nodes in the target link?* Since the PPR score can be considered as the influence of node  $u$  on some root node [6], it suggests that  $u$  has little structural relationship to both nodes in the target link. This implies that node  $u$  likely has little impact on the pairwise information between both nodes in the target link.

Following this philosophy, for a target link  $(a, b)$ , we filter all nodes  $u \in \mathcal{V} \setminus \{a, b\}$  using the PPR scores of  $u$  relative to both nodes in the target link. Specifically, we remove all nodes where the PPR score is below a threshold  $\eta$  relative to both nodes in the target link. As such, we only keep a node  $u$  if it is related in some capacity to at least one of the nodes in the target link. Similarly to Section 3.3, we treat CN, 1-Hop, and  $>1$ -Hop nodes differently by applying a different threshold for them. The filtered node set for each category of nodes is given by:

$$\hat{\mathcal{N}}_{(a,b)}^\pi = \{u \in \mathcal{N}_{(a,b)}^\pi \mid \text{ppr}(a, u) \geq \eta^\pi, \text{ppr}(b, u) \geq \eta^\pi\}, \quad (9)$$

**Table 1: Dataset statistics. The split ratio is the % of samples for train/validation/test.**

	Cora	Citeseer	Pubmed	ogbl-collab	ogbl-ddi	ogbl-ppa	ogbl-citation2
#Nodes	2,708	3,327	18,717	235,868	4,267	576,289	2,927,963
#Edges	5,278	4,676	44,327	1,285,465	1,334,889	30,326,273	30,561,187
Split Ratio	85/5/10	85/5/10	85/5/10	92/4/4	80/10/10	70/20/10	98/1/1

where  $\hat{\mathcal{N}}_{(a,b)}^\pi$  is the filtered node set for all nodes of the type  $\pi \in \{\text{CN}, 1\text{-Hop}, >1\text{-Hop}\}$  and  $\eta^\pi$  is the corresponding PPR threshold. We corroborate this design in Section 4 by demonstrating that LPFormer can achieve SOTA performance in LP while achieving a faster runtime than the second-best method, NCNC [40], on denser graphs. This is despite the fact that LPFormer can attend to a wider variety of nodes. We further show in Section 4.5 that filtering  $>1\text{-Hop}$  nodes can actually help improve performance. We conjecture that this is because excessive global information can inject too much noise into the pairwise encoding.

### 3.5 LPFormer

We now define the overall framework – LPFormer. The overall procedure is given in Figure 2: **(1)** We first learn node representations from the input adjacency and node features via an MPNN. We note that this step is agnostic to the target link. **(2)** For a target link  $(a, b)$  we extract the nodes to attend to, i.e.  $V_{(a,b)}$ . This is done via the PPR thresholding technique defined in Section 3.4. **(3)** We apply  $L$  layers of attention, using the mechanism defined in Section 3.2. The output is the pairwise encoding  $s(a, b)$ . **(4)** We generate the prediction of the target link using three types of information: the element-wise product of the node representation, the pairwise encoding, and the number of CN, 1-Hop, and  $>1\text{-Hop}$  nodes identified by Eq. 9. The score function is given by:

$$p(a, b) = \sigma \left( \text{MLP} \left( \mathbf{h}_a \odot \mathbf{h}_b \parallel s(a, b) \parallel |\hat{\mathcal{N}}_{(a,b)}^{\text{CN}}| \parallel |\hat{\mathcal{N}}_{(a,b)}^1| \parallel |\hat{\mathcal{N}}_{(a,b)}^{>1}| \right) \right) \quad (10)$$

We demonstrate in Table 3 that the inclusion of the node counts is helpful, as it provides complementary information to the pairwise encoding.

## 4 EXPERIMENTS

In this section, we conduct extensive experiments to validate the effectiveness of LPFormer. Specifically, we attempt to answer the following questions: **(RQ1)** Can LPFormer consistently outperform baseline methods on a variety of different benchmark datasets? **(RQ2)** Is LPFormer able to model a variety of different LP factors? **(RQ3)** Can LPFormer be run efficiently on large dense graphs? We further conduct studies ablating each component of our model and analyzing the effect of the PPR-based threshold on performance.

### 4.1 Experimental Settings

**Datasets.** We include Cora, Citeseer, and Pubmed [42] and ogbl-collab, ogbl-ppa, ogbl-ddi, and ogbl-citation2 [18]. Furthermore, for Cora, Citeseer, and Pubmed we experiment under a single fixed split (see Appendix C.1 for further discussion). The detailed statistics for each dataset are shown in Table 1.

**Baseline Models.** We compare LPFormer against a wide variety of baselines including: CN [33], AA [2], RA [49], GCN [25],

SAGE [17], GAE [24], SEAL [45], NBFNet [50], Neo-GNN [44], BUDDY [9], and NCNC [40]. Results on Cora, Citeseer, and Pubmed are taken from Li et al. [27]. Results for the heuristic methods are from Hu et al. [18]. All other results are either from their respective study or Chamberlain et al. [9].

**Evaluation Metrics.** Each positive target link is evaluated against a set of given negative links. The rank of the positive link among the negatives is used to evaluate performance. The two types of metrics that are used to evaluate this ranking are: Hits@K and MRR. For the OGB datasets we use the metric used in the original study. This includes Hits@50 for ogbl-collab, Hits@100 for ogbl-ppa and MRR for ogbl-citation2. Lastly, for Cora, Citeseer, Pubmed we follow Li et al. [27] and use MRR. Lastly, we note that the same set of negative links is used for all positive links except on ogbl-citation2, where [18] provides a customized set of 1000 negatives for each individual positive link.

Additional experimental settings can be found in Appendix D.1.

### 4.2 Main Results

We present the results of LPFormer compared with baselines on multiple benchmark datasets. Note that we omit ogbl-ddi from the main results due to recent issues discovered by Li et al. [27] (see Appendix C.2 for more details). The results are shown in Table 2. We observe that LPFormer can achieve SOTA performance on 5/6 datasets, significantly outperforming other baselines. Moreover, LPFormer is also the most consistent of all the methods, achieving strong performance on all datasets. This is as opposed to previous SOTA methods, NCNC and BUDDY, which tend to struggle on Cora and Pubmed. We attribute the consistency of LPFormer to the flexibility of our model, allowing it to customize the LP factors needed to each link and dataset.

### 4.3 Performance by LP Factor

In this section, we measure the ability of different methods to capture a variety of different LP factors. To measure this, we identify all positive target links **when there is only one dominant LP factor**. For example, one group would contain all target links where the only dominant factor is the local structural information. We focus on links that correspond to one of the three groups identified in [29]: local structural information, global structural information, and feature proximity.

We identify these groups by using popular heuristics as proxies for each factor. For local structural information we use CNs [33], for global structural information we use PPR [6] as it’s the most computationally efficient of all global methods, and for feature proximity we use the cosine similarity of the features. Using these heuristics, we determine if only one factor is dominant by comparing the relative score of each heuristic. This is done by first computing the

**Table 2: Results on benchmark datasets. OOM is an out of memory error. Colored are the results ranked first, second, and third.**

	Cora	Citeseer	Pubmed	ogbl-collab	ogbl-ppa	ogbl-citation2
Metric	MRR	MRR	MRR	H@50	H@100	MRR
CN	20.99 ±0.00	28.34 ±0.00	14.02 ±0.00	56.44 ±0.00	27.65 ±0.00	51.47 ±0.00
AA	31.87 ±0.00	29.37 ±0.00	16.66 ±0.00	64.35 ±0.00	32.45 ±0.00	51.89 ±0.00
RA	30.79 ±0.00	27.61 ±0.00	15.63 ±0.00	64.00 ±0.00	49.33 ±0.00	51.98 ±0.00
GCN	32.50 ±6.87	50.01 ±6.04	19.94 ±4.24	44.75 ±1.07	18.67 ±1.32	84.74 ±0.21
SAGE	<b>37.83 ±7.75</b>	47.84 ±6.39	22.74 ±5.47	48.10 ±0.81	16.55 ±2.40	82.60 ±0.36
GAE	29.98 ±3.21	<b>63.33 ±3.14</b>	16.67 ±0.19	OOM	OOM	OOM
SEAL	26.69 ±5.89	39.36 ±4.99	<b>38.06 ±5.18</b>	64.74 ±0.43	48.80 ±3.16	<b>87.67 ±0.32</b>
NBFNet	<b>37.69 ±3.97</b>	38.17 ±3.06	<b>44.73 ±2.12</b>	OOM	OOM	OOM
Neo-GNN	22.65 ±2.60	53.97 ±5.88	31.45 ±3.17	57.52 ±0.37	49.13 ±0.60	87.26 ±0.84
BUDDY	26.40 ±4.40	59.48 ±8.96	23.98 ±5.11	<b>65.94 ±0.58</b>	<b>49.85 ±0.20</b>	87.56 ±0.11
NCNC	29.01 ±3.83	<b>64.03 ±3.67</b>	25.70 ±4.48	<b>66.61 ±0.71</b>	<b>61.42 ±0.73</b>	<b>89.12 ±0.40</b>
<b>LPFormer</b>	<b>39.42 ±5.78</b>	<b>65.42 ±4.65</b>	<b>40.17 ±1.92</b>	<b>68.03 ±0.46</b>	<b>63.32 ±0.63</b>	<b>89.81 ±0.13</b>

score for each factor  $i$  and target link  $(a, b)$ ,  $s^i(a, b)$ . For each factor, we then compute the score corresponding to the  $p$ -th percentile among all links,  $\hat{s}^i$ . We choose a larger value of  $p$  (i.e. 90%) such that a score  $\geq \hat{s}^i$  indicates that a significant amount of pairwise information exists for that factor. For a single target link, we then compare the score of each factor  $s^i(a, b)$  to  $\hat{s}^i$ . If  $s^i(a, b) \geq \hat{s}^i$  is true **for only one factor**, this implies that the score for only one factor is “high”. Therefore there is a notable amount of pairwise information existing for only one factor for the link  $(a, b)$ . This ensures that only one factor is strongly expressed. If this is true, we then assign the target link  $(a, b)$  to factor  $i$ . Please see Appendix D.3 for a more detailed explanation.

We demonstrate the results on Cora, Citeseer, and ogbl-collab in Figure 3. We observe that LPFormer typically performs best for each individual LP factor on all datasets. Furthermore, it is also the most consistently well-performing on each factor as compared to other methods. For example, on Cora the other methods struggle for links that correspond to the feature proximity factor. LPFormer, on the other hand, is able to significantly outperform them on those target links, performing around 33% better than the second best method. Lastly, we note that most methods tend to perform well on the links corresponding to the global factor, even if they don’t explicitly model such information. This is caused by a strong correlation that tends to exist between local and global structural information, often resulting in considerable overlap between both factors [29]. These results show that LPFormer can indeed adapt to multiple types of LP factors, as it can consistently perform well on samples belonging to a variety of different LP factors. Additional results are given in Appendix D.4.

#### 4.4 Ablation Study

We further include an ablation study to verify the effectiveness of the proposed components in LPFormer. In particular, we introduce 6 variants of LPFormer. (a) **w/o Learnable Att**: No attention is learned. As such, we set all attention weights to 1 and remove the RPE. (b) **w/o Features in Att**: We remove the node feature

information from the attention mechanism. (c) **w/o RPE in Att**: We remove the RPE from the attention mechanism. (d) **w/o PPR RPE**: We replace the PPR-based RPE with a learnable embedding for each of CN, 1-Hop, and >1-Hop nodes. (e) **w/o PPR RPE by Node Type**: We don’t fit a separate function for each node type when determining the PPR RPE (see Section 3.3). Instead we use one for all nodes. (f) **w/o Counts**: We remove the counts of different nodes from the scoring function.

The results are shown in Table 3. We include ogbl-collab, Pubmed, and Citeseer. We observe that ablating each component tends to decrease the performance. However, the magnitude of the decrease is dataset-dependent. For example, on ogbl-collab, ablating the feature information in the attention does not affect the performance. However, on Pubmed and Citeseer, removing the feature information results in a large decrease in performance. We further verify the importance of splitting the nodes into different categories (i.e., CN, 1-Hop, >1-Hop) when computing the RPE. When they aren’t split and only one function is used to encode the PPR scores, the performance drops on each dataset.

**Table 3: Ablation Study on LPFormer**

Method	ogbl-collab	Pubmed	Citeseer
w/o Learnable Att	65.05±0.50	27.72±2.74	56.23±1.75
w/o Features in Att	<b>68.04±0.79</b>	36.12±4.32	53.40±9.30
w/o RPE in Att	65.26±0.56	26.51±3.67	56.70±3.79
w/o PPR RPE	67.09±0.51	28.52±1.18	51.96±15.2
w/o PPR RPE by Node Type	67.95±0.54	33.80±4.24	57.40±5.71
w/o Counts	67.75±0.41	33.12±10.7	54.39±5.30
LPFormer	<b>68.03±0.46</b>	<b>40.17±1.92</b>	<b>65.42±4.65</b>

#### 4.5 Effect of PPR Threshold

We examine the effect of the PPR threshold for including nodes >1 hops away from either node in the target link ( $\eta^{>1}$  in Eq. (9)). Results for Cora, Citeseer, and Pubmed are in Figure 4. We have

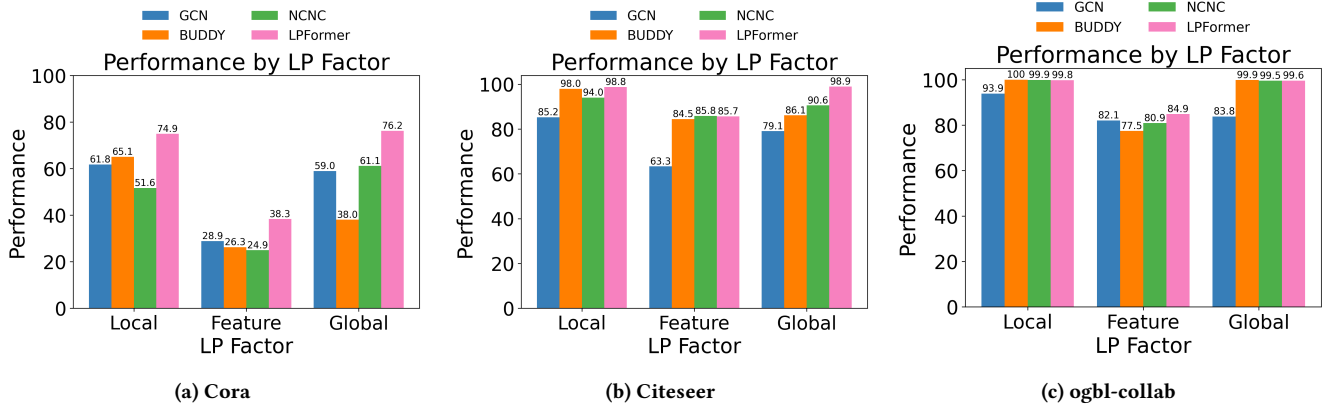


Figure 3: Performance for target links when there is only one LP factor strongly expressed. Results are on (a) Cora, (b) Citeseer, and (c) ogbl-collab.

multiple observations. The first is that not all datasets benefit from the inclusion of global information. Citeseer achieves the best performance when filtering all nodes >1 hops away. Second, is that even when global information is helpful, it is not necessarily optimal to include all nodes >1-Hop away. This is because many nodes >1-Hop away likely have little impact on the target link, thereby introducing noise into the attention. As such, we don't want to consider those nodes when computing the pairwise encoding. These observations underscore the importance of filtering which nodes to attend to irrespective of efficiency, as different sets of information may be needed to model each dataset effectively.

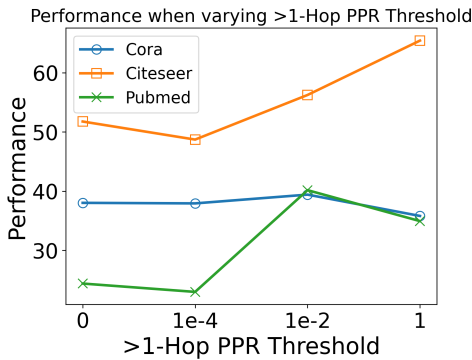


Figure 4: Performance when varying the PPR threshold for >1-Hop nodes.

#### 4.6 Runtime Analysis

In this section, we compare the runtime of LPFormer against NCNC, which is the strongest performing baseline. To obtain a fair comparison we use the same batch size, hidden dimension size, and number of message-passing layers on each dataset for both methods. The results are shown in Figure 5 on all four OGB datasets<sup>1</sup>. We further

<sup>1</sup>We note that we include ogbl-ddi simply as a means of comparing the runtime of our methods. We omit it from the main results. See Appendix C.2 for more discussion.

include the mean degree of each dataset in parentheses. We observe that LPFormer shines on denser datasets, taking significantly less time to train one epoch. This is despite that LPFormer can attend to nodes beyond the 1-hop radius of the target link. This underscores the importance of the PPR thresholding technique introduced in Section 3.4, as it allows for efficient attention to a wider variety of nodes.

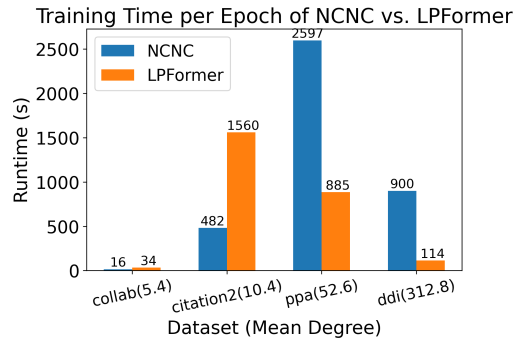


Figure 5: Runtime Comparison of training time of 1 epoch between LPFormer and NCNC. The mean degree is in parentheses.

## 5 CONCLUSION

In this paper we introduce a new framework, LPFormer, that aims to integrate a wider variety of pairwise information for link prediction. LPFormer does this via a specially designed graph transformer, which considers how a node pair relate to each other in the context of the graph. It further works in a adaptive manner, allowing the type of pairwise information to be customized to each target link. Extensive experiments demonstrate that LPFormer can achieve SOTA performance on a wide variety of benchmark datasets while retaining efficiency. We further demonstrate LPFormer's supremacy at modeling multiple types of LP factors. For future work, we plan on exploring other methods of incorporating multiple LP factors with an emphasis on global structural information. We also plan



on evaluating our method on the new harder evaluation setting proposed by [27].

## REFERENCES

- [1] Khushnood Abbas, Alireza Abbasi, Shi Dong, Ling Niu, Laihang Yu, Bolun Chen, Shi-Min Cai, and Qambar Hasan. 2021. Application of network link prediction in drug discovery. *BMC bioinformatics* 22 (2021), 1–21.
- [2] Lada A Adamic and Eytan Adar. 2003. Friends and neighbors on the web. *Social networks* 25, 3 (2003), 211–230.
- [3] Reid Andersen, Fan Chung, and Kevin Lang. 2006. Local graph partitioning using pagerank vectors. In *2006 47th Annual IEEE Symposium on Foundations of Computer Science (FOCS'06)*. IEEE, 475–486.
- [4] Dzmitry Bahdanau, Kyung Hyun Cho, and Yoshua Bengio. 2015. Neural machine translation by jointly learning to align and translate. In *3rd International Conference on Learning Representations, ICLR 2015*.
- [5] Albert-László Barabási, Hawoong Jeong, Zoltan Néda, Erzsébet Ravasz, Andras Schubert, and Tamas Vicsek. 2002. Evolution of the social network of scientific collaborations. *Physica A: Statistical mechanics and its applications* 311, 3-4 (2002), 590–614.
- [6] Sergey Brin and Lawrence Page. 1998. The anatomy of a large-scale hypertextual web search engine. *Computer networks and ISDN systems* 30, 1-7 (1998), 107–117.
- [7] Andrei Z Broder. 1997. On the resemblance and containment of documents. In *Proceedings. Compression and Complexity of SEQUENCES 1997 (Cat. No. 97TB100171)*. IEEE, 21–29.
- [8] Shaked Brody, Uri Alon, and Eran Yahav. 2022. How Attentive are Graph Attention Networks?. In *International Conference on Learning Representations*. <https://openreview.net/forum?id=F72ximsx7C1>
- [9] Benjamin Paul Chamberlain, Sergey Shirobokov, Emanuele Rossi, Fabrizio Frasca, Thomas Markovich, Nils Hammerla, Michael M Bronstein, and Max Hansmire. 2022. Graph Neural Networks for Link Prediction with Subgraph Sketching. *arXiv preprint arXiv:2209.15486* (2022).
- [10] Jinsong Chen, Kaiyuan Gao, Gaichao Li, and Kun He. 2022. NAGphormer: A tokenized graph transformer for node classification in large graphs. In *The Eleventh International Conference on Learning Representations*.
- [11] Fan Chung. 2007. The heat kernel as the pagerank of a graph. *Proceedings of the National Academy of Sciences* 104, 50 (2007), 19735–19740.
- [12] Gonçalo M Correia, Vlad Niculae, and André FT Martins. 2019. Adaptively Sparse Transformers. In *Proceedings of the 2019 Conference on Empirical Methods in Natural Language Processing (EMNLP-IJCNLP)*. 2174–2184.
- [13] Nur Nasuha Daud, Siti Hafizah Ab Hamid, Muntadher Saadon, Firdaus Sahran, and Nor Badrul Anuar. 2020. Applications of link prediction in social networks: A review. *Journal of Network and Computer Applications* 166 (2020), 102716.
- [14] Yuxiao Dong, Reid A Johnson, Jian Xu, and Nitesh V Chawla. 2017. Structural diversity and homophily: A study across more than one hundred big networks. In *Proceedings of the 23rd ACM SIGKDD International Conference on Knowledge Discovery and Data Mining*. 807–816.
- [15] Philippe Flajolet, Éric Fusy, Olivier Gandouet, and Frédéric Meunier. 2007. Hyperloglog: the analysis of a near-optimal cardinality estimation algorithm. *Discrete mathematics & theoretical computer science* Proceedings (2007).
- [16] Justin Gilmer, Samuel S Schoenholz, Patrick F Riley, Oriol Vinyals, and George E Dahl. 2017. Neural message passing for quantum chemistry. In *International conference on machine learning*. PMLR, 1263–1272.
- [17] Will Hamilton, Zhitao Ying, and Jure Leskovec. 2017. Inductive representation learning on large graphs. *Advances in neural information processing systems* 30 (2017).
- [18] Weihua Hu, Matthias Fey, Marinka Zitnik, Yuxiao Dong, Hongyu Ren, Bowen Liu, Michele Catasta, and Jure Leskovec. 2020. Open graph benchmark: Datasets for machine learning on graphs. *Advances in neural information processing systems* 33 (2020), 22118–22133.
- [19] Hong Huang, Jie Tang, Lu Liu, JarDer Luo, and Xiaoming Fu. 2015. Triadic closure pattern analysis and prediction in social networks. *IEEE Transactions on Knowledge and Data Engineering* 27, 12 (2015), 3374–3389.
- [20] Zan Huang, Xin Li, and Hsinchun Chen. 2005. Link prediction approach to collaborative filtering. In *Proceedings of the 5th ACM/IEEE-CS joint conference on Digital libraries*. 141–142.
- [21] Leo Katz. 1953. A new status index derived from sociometric analysis. *Psychometrika* 18, 1 (1953), 39–43.
- [22] Jinwoo Kim, Dat Nguyen, Seonwoo Min, Sungjun Cho, Moontae Lee, Honglak Lee, and Seunghoon Hong. 2022. Pure transformers are powerful graph learners. *Advances in Neural Information Processing Systems* 35 (2022), 14582–14595.
- [23] Thomas N Kipf and Max Welling. 2016. Semi-supervised classification with graph convolutional networks. *arXiv preprint arXiv:1609.02907* (2016).
- [24] Thomas N Kipf and Max Welling. 2016. Variational graph auto-encoders. *arXiv preprint arXiv:1611.07308* (2016).
- [25] Thomas N. Kipf and Max Welling. 2017. Semi-Supervised Classification with Graph Convolutional Networks. In *International Conference on Learning Representations (ICLR)*.
- [26] Devin Kreuzer, Dominique Beaini, Will Hamilton, Vincent Létourneau, and Prudencio Tossou. 2021. Rethinking graph transformers with spectral attention. *Advances in Neural Information Processing Systems* 34 (2021), 21618–21629.
- [27] Juanhui Li, Harry Shomer, Haitao Mao, Shenglai Zeng, Yao Ma, Neil Shah, Jiliang Tang, and Dawei Yin. 2023. Evaluating Graph Neural Networks for Link Prediction: Current Pitfalls and New Benchmarking. *arXiv preprint arXiv:2306.10453* (2023).
- [28] David Liben-Nowell and Jon Kleinberg. 2003. The link prediction problem for social networks. In *Proceedings of the twelfth international conference on Information and knowledge management*. 556–559.
- [29] Haitao Mao, Juanhui Li, Harry Shomer, Bingheng Li, Wenqi Fan, Yao Ma, Tong Zhao, Neil Shah, and Jiliang Tang. 2023. Revisiting Link Prediction: A Data Perspective. *arXiv:2310.00793 [cs.SI]*
- [30] Sameen Maruf, André FT Martins, and Gholamreza Haffari. 2019. Selective Attention for Context-aware Neural Machine Translation. In *Proceedings of NAACL-HLT*. 3092–3102.
- [31] Luis Müller, Mikhail Galkin, Christopher Morris, and Ladislav Rampásek. 2023. Attending to graph transformers. *arXiv preprint arXiv:2302.04181* (2023).
- [32] Yohsuke Murase, Hang-Hyun Jo, János Török, János Kertész, and Kimmo Kaski. 2019. Structural transition in social networks: The role of homophily. *Scientific reports* 9, 1 (2019), 4310.
- [33] Mark EJ Newman. 2001. Clustering and preferential attachment in growing networks. *Physical review E* 64, 2 (2001), 025102.
- [34] Maximilian Nickel, Xueyan Jiang, and Volker Tresp. 2014. Reducing the rank in relational factorization models by including observable patterns. *Advances in Neural Information Processing Systems* 27 (2014).
- [35] Adam Paszke, Sam Gross, Francisco Massa, Adam Lerer, James Bradbury, Gregory Chanan, Trevor Killeen, Zeming Lin, Natalia Gimelshein, Luca Antiga, et al. 2019. Pytorch: An imperative style, high-performance deep learning library. *Advances in neural information processing systems* 32 (2019).
- [36] Ladislav Rampásek, Michael Galkin, Vijay Prakash Dwivedi, Anh Tuan Luu, Guy Wolf, and Dominique Beaini. 2022. Recipe for a general, powerful, scalable graph transformer. *Advances in Neural Information Processing Systems* 35 (2022), 14501–14515.
- [37] Balasubramaniam Srinivasan and Bruno Ribeiro. 2019. On the Equivalence between Positional Node Embeddings and Structural Graph Representations. In *International Conference on Learning Representations*.
- [38] Ashish Vaswani, Noam Shazeer, Niki Parmar, Jakob Uszkoreit, Llion Jones, Aidan N Gomez, Łukasz Kaiser, and Illia Polosukhin. 2017. Attention is all you need. *Advances in neural information processing systems* 30 (2017).
- [39] Petar Velickovic, Guillem Cucurull, Arantxa Casanova, Adriana Romero, Pietro Lio, and Yoshua Bengio. 2017. Graph attention networks. *stat* 1050 (2017), 20.
- [40] Xiyuan Wang, Haotong Yang, and Muhan Zhang. 2023. Neural Common Neighbor with Completion for Link Prediction. *arXiv preprint arXiv:2302.00890* (2023).
- [41] Qitian Wu, Wentao Zhao, Zenan Li, David P Wipf, and Junchi Yan. 2022. Nodeformer: A scalable graph structure learning transformer for node classification. *Advances in Neural Information Processing Systems* 35 (2022), 27387–27401.
- [42] Zhilin Yang, William Cohen, and Ruslan Salakhudinov. 2016. Revisiting semi-supervised learning with graph embeddings. In *International conference on machine learning*. PMLR, 40–48.
- [43] Chengxuan Ying, Tianle Cai, Shengjie Luo, Shuxin Zheng, Guolin Ke, Di He, Yanming Shen, and Tie-Yan Liu. 2021. Do transformers really perform badly for graph representation? *Advances in Neural Information Processing Systems* 34 (2021), 28877–28888.
- [44] Seongjun Yun, Seoyoon Kim, Junhyun Lee, Jaewoo Kang, and Hyunwoo J Kim. 2021. Neo-gnns: Neighborhood overlap-aware graph neural networks for link prediction. *Advances in Neural Information Processing Systems* 34 (2021), 13683–13694.
- [45] Muhan Zhang and Yixin Chen. 2018. Link prediction based on graph neural networks. *Advances in neural information processing systems* 31 (2018).
- [46] Muhan Zhang, Pan Li, Yinglong Xia, Kai Wang, and Long Jin. 2021. Labeling trick: A theory of using graph neural networks for multi-node representation learning. *Advances in Neural Information Processing Systems* 34 (2021), 9061–9073.
- [47] Muhan Zhang, Pan Li, Yinglong Xia, Kai Wang, and Long Jin. 2021. Labeling trick: A theory of using graph neural networks for multi-node representation learning. *Advances in Neural Information Processing Systems* 34 (2021), 9061–9073.
- [48] He Zhao, Lan Du, and Wray Buntine. 2017. Leveraging node attributes for incomplete relational data. In *International conference on machine learning*. PMLR, 4072–4081.
- [49] Tao Zhou, Linyuan Lü, and Yi-Cheng Zhang. 2009. Predicting missing links via local information. *The European Physical Journal B* 71 (2009), 623–630.
- [50] Zhaocheng Zhu, Zuobai Zhang, Louis-Pascal Xhonneux, and Jian Tang. 2021. Neural bellman-ford networks: A general graph neural network framework for link prediction. *Advances in Neural Information Processing Systems* 34 (2021), 29476–29490.

## A EXISTING FORMULATIONS OF PAIRWISE ENCODINGS

In this section we give an overview of existing formulations of pairwise encodings using in DP-MPNNs. The standard formulation of DP-MPNNs is given in Eq. 1 where  $s(a, b)$  is the pairwise encoding. We briefly describe other existing solutions below:

**NCNC** [40]: NCN only considers the CNs of the target link  $(a, b)$  by summing the node representation of each. The pairwise encoding,  $s(a, b)$ , is written as:

$$s(a, b) = \sum_{u \in \mathcal{N}^{\text{CN}}} \mathbf{h}_u, \quad (11)$$

where  $\mathbf{h}_u$  is the node representation encoded by a MPNN.

**NCNC** [40]: NCNC extends NCN by further considering the 1-hop neighbors of the node pair that aren't CNs. To account for the difference, they are weighted by the probability of they themselves being CNs of the other node in the pair. This is given for a target link  $(a, b)$  as:

$$s(a, b) = \sum_{u \in \mathcal{V}} w(a, b, u) \mathbf{h}_u, \quad (12)$$

where

$$w(a, b, u) = \begin{cases} 1, & \text{when } u \in \text{CN}(a, b) \\ \text{NCN}(A, X, b, u) & \text{when } u \in \mathcal{N}(a) \\ \text{NCN}(A, X, a, u) & \text{when } u \in \mathcal{N}(b) \\ 0, & \text{else} \end{cases}. \quad (13)$$

This weighting scheme ensures that CNs play a larger role in the pairwise information than non-CN.

**BUDDY** [40]: BUDDY considers counting the number of nodes that correspond to different labels given by the double radius node labeling trick [46]. We first define the number of nodes that are a distance  $d_a$  and  $d_b$  from nodes  $a$  and  $b$  as  $\mathcal{A}_{ab}[d_a, d_b]$ . We further define the number of nodes where  $\max(d_u, d_v) > k$  as  $\beta_{ab}[d]$ . The pairwise encoding concatenates the counts belonging to all combination of  $d = 1 \cdots k$ . The counts are estimated using subgraph sketching algorithms [7, 15] and are denoted  $\hat{\mathcal{A}}$  and  $\hat{\beta}$ . The pairwise encoding for a target link  $(a, b)$  is given by the following where  $[k] = \{1 \cdots k\}$ :

$$s^{\hat{\mathcal{A}}}(a, b) = \prod_{d_a, d_b \in [k]} \hat{\mathcal{A}}_{ab}[d_a, d_b], \quad (14)$$

$$s^{\hat{\beta}}(a, b) = \prod_{d \in [k]} \hat{\beta}_{ab}[d], \quad (15)$$

$$s(a, b) = s^{\hat{\mathcal{A}}}(a, b) \parallel s^{\hat{\beta}}(a, b). \quad (16)$$

**Neo-GNN** [40]: Neo-GNN considers the higher-order neighbor overlap between two nodes. This is done by first learning a structural representation for each node  $i$ ,  $x_i^{\text{struct}}$ . This is given by:

$$x_i^{\text{struct}} = f_1 \left( \sum_{j \in \mathcal{N}(i)} f_2(A_{ij}) \right). \quad (17)$$

To consider the  $L$ -hop structural information, the structural representations are diffused over  $L$  hops and weighted by a hyperparameter  $\beta$ :

$$Z = \text{MLP} \left( \sum_{l=1}^L \beta^{l-1} A^l X^{\text{struct}} \right), \quad (18)$$

$$\text{where } X = \text{diag}(x^{\text{struct}}). \quad (19)$$

The pairwise encoding  $s(a, b)$  is the dot product of both the final representations,

$$s(a, b) = z_a^T z_b. \quad (20)$$

## B SPECIAL CASES OF THE GENERAL PAIRWISE ENCODING

In this section we demonstrate that multiple popular heuristics and pairwise encodings can be formulated as special cases of the general pairwise encoding given in Eq. (2).

**Common Neighbors (CNs)** [33]: The CNs of a pair of nodes  $(a, b)$  is defined the overlapping 1-hop neighbors of both nodes:

$$\text{CN}(a, b) = \mathcal{N}(a) \cap \mathcal{N}(b). \quad (21)$$

Eq. (2) is equal to the CNs when  $h(a, b, u) = 1$  and  $w(a, b, u)$  is:

$$w(a, b, u) = \begin{cases} 1, & \text{when } u \in \mathcal{N}(a) \cap \mathcal{N}(b) \\ 0, & \text{else} \end{cases}. \quad (22)$$

**Adamic-Adar (AA)** [2]: AA is defined as the reciprocal log-degree weighted CN score where  $d_u$  is the degree of node  $u$ :

$$AA(a, b) = \sum_{u \in \text{CN}(a, b)} \frac{1}{\log(d_u)}. \quad (23)$$

Eq. (2) can be rewritten as the AA when  $h(a, b, u) = 1/\log(d_u)$  and  $w(a, b, u)$  is equal to Eq. (22).

**Resource Allocation (RA)** [49]: RA is defined as the reciprocal degree weighted CN score:

$$RA(a, b) = \sum_{u \in \text{CN}(a, b)} \frac{1}{d_u}. \quad (24)$$

Eq. (2) can be rewritten as the AA when  $h(a, b, u) = 1/d_u$  and  $w(a, b, u)$  is equal to Eq. (22).

**Katz Index** [21]: The Katz index is a global structural measure. It is defined as weighted summation of the number of paths of different lengths connecting  $a$  and  $b$ . It is given by the following where the decay weight  $\beta \in [0, 1]$ ,

$$\text{Katz}(a, b) = \sum_{l=1}^{\infty} \beta^l A^l_{a,b}. \quad (25)$$

This is equivalent to Eq. (2) when:

$$w(a, b, u) = \sum_{l=1}^{\infty} \beta^l e_a^T A^l, \quad (26)$$

where  $e_i \in \mathbb{B}^{|\mathcal{V}|}$  is a one-hot vector for a node  $i$ . We further set,

$$h(a, b, u) = \begin{cases} e_b^T, & \text{when } u = b \\ \mathbf{0}, & \text{else} \end{cases}. \quad (27)$$

**Personalized Pagerank (PPR) Score** [6]: The personalized pagerank score is the pagerank score localized to a root node  $u$ . The localization is via a teleportation probability  $\alpha$  that transports the random walk back to the root node. We show that Eq. (2) can be rewritten as the PPR score when setting  $h(a, b, u)$  equal to (27) and, following Chung [11], setting  $w(a, b, u)$  to:

$$w(a, b, u) = \alpha \sum_{l=0}^{\infty} (1 - \alpha)^l e_a^T (D^{-1}A)^l. \quad (28)$$

**Feature Similarity**: The feature similarity of the pair of nodes  $(a, b)$  is expressed by  $\text{dis}(\mathbf{x}_a, \mathbf{x}_b)$  where  $\mathbf{x}_a$  are the node features of node  $a$  and  $\text{dis}(\cdot)$  is a distance function (e.g., euclidean distance). This can be rewritten as Eq. (2) by substituting:

$$w(a, b, u) = \text{dis}(\mathbf{x}_a, \mathbf{x}_u), \quad (29)$$

and  $h(a, b, u) = e_b^T$  where  $e_i \in \mathbb{B}^{|\mathcal{V}|}$  is a one-hot vector for a node  $i$ .

**NCN** [40]: The pairwise encoding used in NCN is defined as the summation of the representations for the CNs of a link. Eq. (2) can be rewritten as NCN when  $w(a, b, u)$  is equal to Eq. (22).  $h(a, b, u)$  is equal to the node representation  $u$  encoded by a MPNN, i.e.,  $h(a, b, u) = \mathbf{h}_u$  where  $H = \text{MPNN}(A, X)$ .

**NCNC** [40]: NCNC extends NCNC by further weighting the 1-hop (non-CN) by their probability of linking to the other nodes. Given Eq. (2), the weight  $w(a, b, u)$  is equal to following where 1-hop neighbors are weighted by their probability of linking with the other node:

$$w(a, b, u) = \begin{cases} 1, & \text{when } u \in \text{CN}(a, b) \\ \text{NCN}(A, X, b, u) & \text{when } u \in \mathcal{N}(a) \\ \text{NCN}(A, X, a, u) & \text{when } u \in \mathcal{N}(b) \\ 0, & \text{else} \end{cases}. \quad (30)$$

$\text{NCN}(A, X, a, u)$  is the probability of  $a$  and  $u$  being linked using the NCN model. We further define  $h(a, b, u) = \mathbf{h}_u$ .

**Neo-GNN** [44]: The pairwise encoding used in Neo-GNN considers the higher-order neighborhood overlap between two nodes. The formulation is given in Section B. When  $l = 1$ , it can be expressed using Eq. (2) by setting:

$$h(a, b, u) = f_1 \left( \sum_{v \in \mathcal{N}(u)} f_2(A_{uv}) \right)^2, \quad (31)$$

and

$$w(a, b, u) = \begin{cases} 1, & \text{when } u \in \overline{\mathcal{N}^{\text{CN}}} \\ 0, & \text{else} \end{cases}. \quad (32)$$

## C PROOF OF PROPOSITION 1

**Proposition 1.** Consider a target link  $(a, b)$  and a node  $u \in \mathcal{V} \setminus \{a, b\}$ . The PPR [6] score of a root node  $i$  and target node  $j$  with teleportation probability  $\alpha$  is denoted by  $\text{ppr}(i, j)$ . Let  $r_a^k(u)$  be the number of walks of length  $k$  that begin at node  $a$  and terminate at  $u$ . We define  $r_{a,b}^k(u) := r_a^k(u) + r_b^k(u)$ . We also define a weight  $\gamma^k := \alpha(1 - \alpha)^k$  for all walks of length  $k$ . The PPR scores,  $\text{ppr}(a, u)$  and  $\text{ppr}(b, u)$ , along with the aggregate number of walks of disparate lengths, are interconnected through the following relationship.

$$\Gamma(a, b, u) = \text{ppr}(a, u) + \text{ppr}(b, u) = \sum_{k=0}^{\infty} \alpha(1 - \alpha)^k r_{a,b}^k(u). \quad (6)$$

PROOF. Per Chung [11], the PPR vector for a root node  $s$ ,  $\text{pr}_s$ , is equivalent to:

$$\text{pr}_s = \alpha \sum_{k=0}^{\infty} (1 - \alpha)^k W^k x_s, \quad (33)$$

where  $W$  is a the random walk matrix and  $x_s$  is a preference vector that is a one-hot vector for element  $s$ . We note that  $\text{pr}_s(t)$  represents the landing probability of node  $t$  given the root node  $s$ . As such, by definition,  $\text{pr}_s(t) = \text{ppr}(s, t)$ . Furthermore, it is clear that  $r_s^k = W^k x_s \in \mathbb{R}^{\mathcal{V}}$  represents the number of walks of length  $k$  that begin at  $s$  and stop all other nodes, individually. Also all walks of length  $k$  are weighted by  $\gamma^k = \alpha(1 - \alpha)^k$ .

$\Gamma(a, b, u)$  can be obtained by first taking the sum of the PPR vectors for nodes  $a$  and  $b$ ,

$$\begin{aligned} \text{pr}_a + \text{pr}_b &= \alpha \sum_{k=0}^{\infty} (1 - \alpha)^k W^k x_a + \alpha \sum_{k=0}^{\infty} (1 - \alpha)^k W^k x_b, \\ \text{pr}_{a,b} &= \alpha \sum_{k=0}^{\infty} (1 - \alpha)^k W^k (x_a + x_b), \end{aligned} \quad (34)$$

where  $\text{pr}_{a,b} = \text{pr}_a + \text{pr}_b$ . From this, we can express  $\Gamma(a, b, u)$  as:

$$\begin{aligned} \Gamma(a, b, u) &= \text{ppr}(a, u) + \text{ppr}(b, u), \\ &= \text{pr}_{a,b}(u), \\ &= \text{pr}_a(u) + \text{pr}_b(u), \end{aligned} \quad (35)$$

which as shown in Eq. (34) is equivalent to the number of combined weighted walks that originate from nodes  $a$  or  $b$  and terminates at node  $u$ . This completes the proof.  $\square$

### C.1 Planetoid splits

We note that for each of Cora, Citeseer, Pubmed we use a fixed split. This follows the recent work of [27]. Li et al. [27] observe that for Cora, Citeseer, Pubmed there exists no unified data split between studies. They find that while recent work [9, 40] use 10 random splits, prior work [39, 50] use a fixed split and train over 10 random seeds. Furthermore, there exists discrepancies in the preprocessing between those works that use the random splits. Chamberlain et al. [9] only use the largest connected component of each dataset while Wang et al. [40] use the whole dataset. This makes any comparison of the published results difficult. Due to these discrepancies, we use the performance on the fixed split given by Li et al. [27], as *it's the only split where all methods are evaluated and compared under the same setting*.

### C.2 Omission of ogbl-ddi

We further omit the results of ogbl-ddi in Table 2. This is due to the observation made by Li et al. [27] that there exists a poor relationship between the validation and test performance. This extends to recent pairwise MPNNs, including NCN [40], Neo-GNN [44], and BUDDY [9]. This makes tuning on the validation set difficult, as it doesn't guarantee good test performance. Due to this, they observe that when tuning on a fixed set of hyperparameter ranges, they are unable to achieve comparable results to the reported performance. Often they observe that the performance is actually much lower. Due to these concerns we believe ogbl-ddi is not suitable for the task of transductive link prediction and don't report the performance. For more details and discussion, please see Appendices C and D in Li et al. [27].

## D ADDITIONAL EXPERIMENTAL DETAILS

### D.1 Additional Experimental Settings

We further discuss the experimental settings used in Section 4.

**Infrastructure:** All experiments were implemented and run using the PyTorch framework [35]. Multiple types of GPUs were used for running the experiments including a 32Gb Tesla V100, a 48Gb Nvidia RTX A6000 48Gb, and a 24Gb NVIDIA RTX A5000. The code is available at <https://github.com/HarryShomer/LPFormer>.

**Hyperparameters:** The learning rate is tuned from  $\{1e^{-3}, 5e^{-3}\}$ , the decay from  $\{0.95, 0.975, 1\}$ , and the dropout from  $[0, 0.7]$ , and the weight decay from  $\{0, 1e^{-4}, 1e^{-7}\}$ . The size of the hidden dimension is set to 64 for ogbl-ppa and ogbl-citation2, 128 for Cora, Pubmed, and ogbl-collab, and 256 for Citeseer. Lastly, the PPR threshold is tuned from  $\{1e^{-2}, 1e^{-3}, 1e^{-4}\}$ .

### D.2 Computation of the PPR Matrix

We compute the PPR matrix via the efficient approximation algorithm introduced by Andersen et al. [3]. The estimation is controlled by a tolerance parameter  $\epsilon$ . The parameter  $\epsilon$  controls both the speed of computation and the sparsity of the solution (i.e., a higher value of  $\epsilon$  will produce a sparser PPR matrix). We use:  $\epsilon = 1e^{-7}$  for Cora and Citeseer,  $\epsilon = 5e^{-5}$  for ogbl-collab and ogbl-ppa,  $\epsilon = 1e^{-5}$  for Pubmed, and  $\epsilon = 5e^{-3}$  for ogbl-Citation2. The value of  $\epsilon$  is chosen as a trade-off between accuracy and sparsity to allow for ease of storage in GPU memory.

### D.3 Splitting Target Links by LP Factor

In Section 4.3 we demonstrate the performance on samples that correspond to a single LP factor. In this section we further detail the algorithm used to determine the set of samples corresponding to each factor. We consider the three main factors: local structural information, global structural information, and feature proximity. We measure each using a single representative heuristic: CNs [33] for local information, PPR [6] for global information, and cosine feature similarity for feature proximity. For each sample, we check if the score is only high in **one** heuristic. In this way, it tells us that there is a dominant factor present in the pairwise information.

This determination is done by comparing the heuristic scores of each target link against a threshold value. For a LP factor  $i$  and target link  $(a, b)$ , we denote the heuristic score as  $s^i(a, b)$ . The threshold value for factor  $i$  is represented by  $\hat{s}^i$  and is chosen such that it corresponds to a higher score. We desire  $\hat{s}^i$  to be a higher score such that any score  $\geq$  than it indicates that a plethora of pairwise information exists corresponding to factor  $i$ . This is done by setting the threshold equal to the  $p$ -th percentile value for that heuristic among all target links. For example, for CNs, the 80th percentile score on one dataset may be 9. The value of  $p$  is chosen to be high (e.g., 80%) due to the aforementioned reasoning. Given these inputs, for each target link we compare the score for factor  $i$  against the threshold value of that factor. Continuing our example, if  $(a, b)$  only has 2 CNs, it is below the previously defined threshold. We only consider a sample as “belonging” to a single factor when it is  $s^i(a, b) \geq \hat{s}^i$  is true **for one only one factor**  $i$ . So if the heuristic score for  $(a, b)$  is below the  $p$ -th percentile threshold for CNs and PPR but above for feature similarity, then feature proximity will be considered the dominant LP factor. However, if it’s above the threshold for both local and structural information, it will not be assigned to any group. This is done as we want to isolate links that only highly express one LP factor. This allows us to better understand how certain methods can model that specific factor. The detailed algorithm is given in Algorithm 1.

We note that each target link may not belong to a category. This can be due to there being no or many dominant LP factor. We further set the percentile equal to 90% on all datasets except for ogbl-collab for which we use 80%. These values were chosen as we wanted the percentile to be suitably high such that we are confident that the corresponding factor is relevant to the target link. Furthermore, we use a lower value for ogbl-collab as we found it produced a more even distribution of links by factor.

### D.4 Additional Results for the LP Factor Experiments

In Section 4.3 we observed the performance of various methods on target links where only a single LP factor is expressed. This is done through the use of heuristic scores. We further demonstrate the results on the Pubmed and ogbl-ppa datasets. Of note is that for ogbl-ppa the initial node features are one-hot vectors that signify the species that the protein belongs to. We observe that due to the sparseness of these features, feature proximity measures are unable to properly predict any target links on their own. As such, the factor corresponding to feature proximity is not expressed. We therefore exclude that factor for this analysis on ogbl-ppa.

The results for both Pubmed and ogbl-ppa datasets are given in Figure 6. As shown earlier in Figure 3, LPFormer can most consistently perform well across each factor. This suggests that LPFormer is best able to both model a variety of factors and adapt accordingly for each target link.

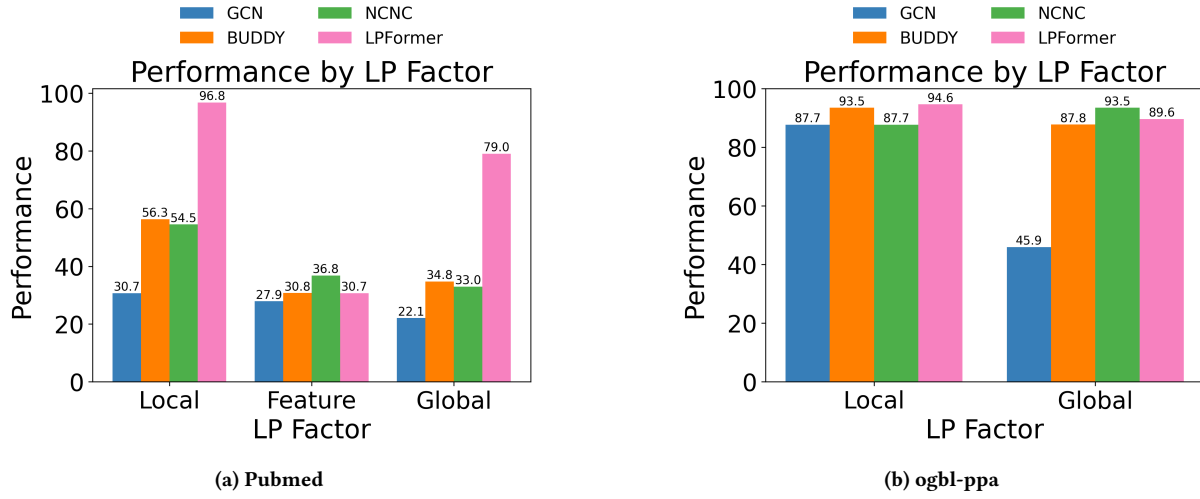


**Figure 6: Performance for target links when there is only one LP factor strongly expressed. Results are on (a) Pubmed, (b) ogbl-ppa. We note that due to the quality of features used, we omit the feature proximity factor for ogbl-ppa from our analysis**

---

Algorithm 1 Determining Samples by LP Factor

---

**Require:**

- $CN(\cdot)$  = Maps  $(i, j)$  to # of CNs of the pair
- $PPR(\cdot)$  = Maps  $(i, j)$  to PPR score of the pair
- $FS(\cdot)$  = Maps  $(i, j)$  to feature cosine similarity of the pair
- $p$  = Percentile used to determine whether a factor is present
- $\mathcal{E}^{\text{test}}$  = Positive test links

```

1: // Compute the score corresponding to the  $p$ -th percentile for each heuristic
2:  $\hat{s}^{\text{CN}} = \text{Percentile}(p, \{CN(i, j) \mid (i, j) \in \mathcal{E}^{\text{test}}\})$ 
3:  $\hat{s}^{\text{FS}} = \text{Percentile}(p, \{FS(i, j) \mid (i, j) \in \mathcal{E}^{\text{test}}\})$ 
4:  $\hat{s}^{\text{PPR}} = \text{Percentile}(p, \{PPR(i, j) \mid (i, j) \in \mathcal{E}^{\text{test}}\})$ 

5: Create empty lists  $L^{\text{CN}}$ ,  $L^{\text{PPR}}$ , and  $L^{\text{FS}}$ 
6: for  $(i, j) \in \mathcal{E}^{\text{test}}$  do
7:   link-cn =  $CN(i, j)$ 
8:   link-fs =  $FS(i, j)$ 
9:   link-ppr =  $PPR(i, j)$ 

10: // Assign sample to corresponding list based on scores
11: if link-cn  $\geq \hat{s}^{\text{CN}}$  and link-fs  $< \hat{s}^{\text{FS}}$  and link-ppr  $< \hat{s}^{\text{PPR}}$  then
12:   Append( $L^{\text{CN}}$ ,  $(i, j)$ )
13: else if link-cn  $< \hat{s}^{\text{CN}}$  and link-fs  $\geq \hat{s}^{\text{FS}}$  and link-ppr  $< \hat{s}^{\text{PPR}}$  then
14:   Append( $L^{\text{FS}}$ ,  $(i, j)$ )
15: else if link-cn  $< \hat{s}^{\text{CN}}$  and link-fs  $< \hat{s}^{\text{FS}}$  and link-ppr  $\geq \hat{s}^{\text{PPR}}$  then
16:   Append( $L^{\text{PPR}}$ ,  $(i, j)$ )
17: end if
18: end for
19: return  $L^{\text{CN}}$ ,  $L^{\text{PPR}}$ ,  $L^{\text{FS}}$ 

```

---